Helicobacter pylori regulates ILK signaling pathways to influence autophagy in gastric epithelial cells

Zheng Xu
Binzhou Medical University
Yunqiu Du
Binzhou Medical University
Ruiqing Zhang
Binzhou Medical University
Xiaohan Tong
Binzhou Medical University
Boqing Li (sdliboqing@163.com)
Binzhou Medical University
Yulong Wu
Binzhou Medical University
Xiaofei Ji
Binzhou Medical University
Ying Zhang (zhangying99g99@163.com)
Binzhou Medical University https://orcid.org/0000-0002-4452-2359

Research

Keywords: ILK, H. pylori, Autophagy, Rac1, RhoA

Posted Date: September 1st, 2020

DOI: https://doi.org/10.21203/rs.3.rs-63602/v1

Abstract

Background

The ability of *Helicobacter pylori* to manipulate host autophagy is an important pathogenic mechanism.

Results

We found a negative correlation between the expression of ILK and the autophagy marker protein LC3B in *H. pylori*-positive human samples and in *H. pylori*-infected GES-1 cell lines. There was a significant accumulation of autophagosomes in ILK-knockdown GES-1 cells, and the expression levels of both LC3B and p62 were also increased. Here, we showed the activities of Rac1 and RhoA were decreased in *H. pylori*-infected GES-1 cells and ILK-knockdown GES-1 cells. Inhibition of Rac1 and RhoA increased LC3B levels and autophagosome formation in GES-1 cells after *H. pylori* infection. Simultaneously, *H. pylori* infection activated downstream signal molecules of Rac1 (PAK1, LIMK1 and cofilin) and RhoA (ROCK1, ROCK2 and LIMK1 and cofilin).

Conclusions

Our results demonstrated that *H. pylori* regulated autophagy through ILK/Rac1 and ILK/RhoA signaling pathways in gastric epithelial cells.

1. Background

Helicobacter pylori resides in more than half of the human population and has co-evolved with humans for more than 58,000 years (Otero et al., 2014). *H. pylori* can evade the host immune defense system, colonize in human gastric mucosa and maintain long-term chronic infection (Dunn et al., 1997). It has evolved cytotoxin-associated gene A (CagA) and vacuolating cytotoxin (VacA) to achieve this purpose (Radosz-Komoniewska et al., 2005). It employs a multicomponent type IV secretion system (T4SS) to secrete CagA into the cytosol of infected host cells and initiate various host responses (Schuelein et al., 2011). In addition to CagA, VacA is identified as necessary and sufficient conditions of *H. pylori* to induce autophagy in gastric epithelial cells (Raju et al., 2012).

Autophagy is an evolutionary conservative process with the degradation of cytoplasmic organelles, proteins, or pathogens in eukaryotic cells (Klionsky and Emr, 2000). Autophagy fuses autophagosomes with lysosomes to form autolysosome, and it is regulated by a variety of autophagy-related genes (Klionsky et al., 2003). Upon bacterial infection, autophagy is induced through host signaling pathways, which results in pathogen being encapsulated within autophagosomes, and then fuses with lysosomes, thereby leading to the degradation of the encapsulated bacteria (Rich et al., 2003). Autophagy as an intracellular defense to eliminate pathogens can be induced by *H. pylori* in gastric epithelial cells (Terebiznik et al., 2009; Tang et al., 2012). However, previous studies have indicated that *H. pylori* could

prevent its degradation, reside and multiply in autophagosomes, and maintain persistent infection (Sit et al., 2020; Wang et al., 2009).

H. pylori T4SS makes a contact with integrin 1 directly that strongly supports the translocation of CagA into the cytosol of infected host cells (Schuelein et al., 2011). Integrin-linked kinase (ILK) plays a central role in the integrin signaling pathway and couples integrin activation to actin cytoskeleton (Ghatak et al., 2013), which transmits extracellular signals to cells and mediates cell growth and differentiation (Grashoff et al., 2012). ILK can activate the family members of Rho GTPases (Graness et al., 2006), which mediate changes in actin polymerization by manipulating the terminal effector protein cofilin-1, leading to the formation of stress fibers, filopodia or lamellipodia, and ruffles (Dedhar, 2000). Previous studies have shown that actin dynamics play a vital role in the whole process of autophagy (Kast and Dominguez, 2017). In this study, we explore the mechanism of *H. pylori* affecting autophagy by regulating ILK.

2. Results

2.1 The ILK expression decreased and the LC3B expression increased duringH. pyloriinfection in gastric epithelial cells

ILK and LC3B, as represented by green fluorescence, were distributed in *H. pylori*-negative or -positive human gastric epithelial cells (Fig. 1a and 1b). The average fluorescence intensity of ILK was markedly decreased ($P < 0.001$) in *H. pylori*-positive human gastric epithelial cells compared with that in *H. pylori*-negative human gastric epithelial cells (Fig. 1c). And the average fluorescence intensity of autophagy marker protein LC3B was significantly higher ($P < 0.001$) in *H. pylori*-positive human gastric epithelial cells than that in *H. pylori*-negative human gastric epithelial cells (Fig. 1d). We speculated that the reduced ILK in human samples could affect the LC3B. Therefore, Pearson's correlation analysis was used to compare the relative levels of ILK and LC3B in these samples. There was statistically a significant negative correlation ($P < 0.001$) between ILK and LC3B only in *H. pylori*-positive human gastric epithelial cells (R = 0.653) (Fig. 1e); this finding indicated that ILK was inversely correlated with LC3B in *H. pylori*-positive human samples.

We also proved that ILK was downregulated and autophagosomes were increaed in GES-1 cell lines after *H. pylori* infection. As shown in Fig. 2a, infection with *H. pylori* with or without CagA decreased ILK phosphorylation in GES-1 cells, and CagA knockout *H. pylori* ($CagA^-$) led lower level of ILK phosphorylation ($P < 0.01$) compared to that caused by *H. pylori* wild type. The total amount and phosphorylated ILK were down-regulated ($P < 0.05$) at 2, 4, 6, and 8 h in GES-1 cells after *H. pylori* challenge (Fig. 2b). The tandem mRFP-GFP-LC3B adenovirus assay is based on the pH difference between the acidic autolysosome and the neutral autophagosome. The progress of autophagosome to autolysosome was manipulated by the differences in pH sensitivity of green fluorescent protein (GFP) and red fluorescent protein (RFP). Once autophagosome and lysosome fused to form autolysosomes, the GFP moiety degraded from the tandem protein, but mRFP-LC3B still maintains the punta. Induction of

autophagosome (merge of GFP-LC3B and mRFP-LC3B) and autolysosome (mRFP-LC3B) formation in GES-1 cells after *H. pylori* infection occurred in a time-dependent manner (Fig. 2c). The numbers of autophagosome increased at 4, 6 and 8 h in GES-1 cells after *H. pylori* infection, and the numbers were the most at 6 h after bacterial infection, and the numbers of autolysosome gradually increased from 2 to 8 h and reached the peak at 6 h in GES-1 cells after *H. pylori* infection (Fig. 2d). The p62 levels decreased at 2 h and increased at 4, 6 and 8 h after *H. pylori* infection ($P < 0.05$) (Fig. 2e). These results further indicated that *H. pylori* disrupted autophagy in GES-1 cells.

2.2 Downregulation of ILK disrupted autophagy in GES-1 cells

RNAi was used to downregulate the expression of ILK in GES-1 cells. Western blot analysis demonstrated that ILK was reduced compared to that in the negative group at 48 h after transfection with sequence-specific siRNA (HSS140843, HSS179923, or HSS179924) targeting ILK (Fig. 3a). Ultimately, we chose HSS140843 as the target siRNA to reduce the expression of ILK for subsequent experiments. To further study the influence of ILK on autophagy in *H. pylori*-infected GES-1 cells, the tandem mRFP-GFP-LC3B adenovirus was used to evaluate the formation of autophagosome and autolysosome. As shown in Fig. 3b and 3c, we found increased formation of yellow fluorescent autophagosomes and red fluorescent autolysomes in ILK-knockdown GES-1 cells compared with those in control siRNA-treated GES-1 cells, regardless of whether or not GES-1 cells were infected by *H. pylori*. The number of autophagosomes were 104.3 ± 7.57 per cell, which was 1.57-fold higher ($P = 0.017$) in ILK knockdown GES-cells after *H. pylori* infection than that in control siRNA-treated GES-1 cells after *H. pylori* infection. To further corroborate the influence of ILK on autophagy, the appearance of double-membraned autophagosomes was investigated by transmission electron microscopy (Fig. 3d). There was a significant accumulation of autophagosomes in ILK-knockdown GES-1 cells compared to that in control siRNA-treated GES-1 cells. The LC3B levels were then assessed by western blot analysis. As shown in Fig. 3e, LC3B was significantly up-regulated ($P < 0.05$) and p62 was significantly down-regulated ($P < 0.05$) in GES-1 cells after *H. pylori* infection. The LC3B and p62 levels were both higher ($P < 0.05$) in ILK-knockdown GES-1 cells than those in control siRNA-treated GES-1 cells after *H. pylori* infection. These results indicated that downregulation of ILK disrupted autophagy in *H. pylori*-infection GES-1 cells.

2.3 Inhibition of ILK influenced Rac1 and RhoA activation in GES-1 cells

Total Rac1 and GTP-Rac1, and total RhoA and GTP-RhoA were detected by western blot. GTP/Total Rac1 and GTP/Total RhoA were decreased in GES-1 cells after *H. pylori* infection and in ILK-knockdown GES-1 cells regardless whether or not GES-1 cells were infected with *H. pylori* (Fig. 4). GTP/Total Rac1 and GTP/Total RhoA were were 3/4-fold ($P < 0.05$) and 2/5-fold ($P < 0.05$) lower in *H. pylori*-infected GES-1 cells than in the blank GES-1 cells, respectively.

2.4 Inhibition of Rac1 and RhoA influenced autophagy in GES-1 cells

The cells survival rates were to detect concentration-dependent and time-dependent toxicity of inhibitors against GES-1 cells. No significant difference was observed in cell survival rate between inhibitor-treated groups (10 and 50 μM of NSC23766, and 2 and 5 μM of CCG-1423-treated GES-1 cells) and blank group. The GES-1 cells treated with 50 μM of NSC23766 and 5 μM of CCG-1423 at 1, 2 and 4 h showed no change in cell survival rates (Fig. 5a). The LC3B levels were assessed by western blot to clarify whether inhibition of Rac1 and RhoA influenced autophagy. As shown in Fig. 5b, LC3B was significantly increased ($P < 0.05$) in Rac1- or RhoA-inhibited GES-1 cells compared to that in control GES-1 cells, regardless of whether the cells were infected with *H. pylori*. To further study the influence of Rac1 and RhoA on autophagy in GES-1 cells, the tandem mRFP-GFP-LC3B adenovirus was used to evaluate the formation of autophagosome and autolysosome. As shown in Fig. 5c and 5d, we found increased formation of yellow fluorescent autophagosomes in *H. pylori*-infected, Rac1- and RhoA-inhibited GES-1 cells with or without *H. pylori* compared to those in control GES-1 cells. The red fluorescent autolysosomes in *H. pylori* alone-infected, Rac1- and RhoA-inhibited GES-1 cells were more ($P < 0.01$) than that in untreated GES-1 cell, but the autolysosomes in Rac1- and RhoA-inhibited GES-1 cells with *H. pylori* infection were remarkably decreased compared to that in GES-1 cells infected by *H. pylori* alone. These results indicated that the inhibition of Rac1 or RhoA only increased autophagosome formation in GES-1 cells after *H. pylori* infection.

2.5 Inhibition of Rac1 and RhoA influenced downstream signaling molecules

To determine whether PAK1, ROCK1, ROCK2, LIMK1, and cofilin were regulated by Rac1 or RhoA, we investigated PAK1, ROCK1, ROCK2, LIMK1, and cofilin mRNA and protein phosphorylation levels in Rac1- or RhoA-inhibited GES-1 cells through qRT-PCR and western blot. The mRNA levels of PAK1, ROCK1, ROCK2 and LIMK1 were significantly higher ($P < 0.05$), and cofilin was remarkably lower ($P < 0.01$) in GES-1 cells after *H. pylori* infection than those in untreated GES-1 cells. The mRNA levels of PAK1 and LIMK1 were significantly decreased ($P < 0.001$) and cofilin was remarkably increased ($P < 0.05$) in NSC23766-treatment GES-1 cells compared to those in untreated GES-1 cells, and the same trends were observed in NSC23766-treatment GES-1 cells after *H. pylori* infection compared to those in *H. pylori*-infected GES-1 cells. The mRNA levels of ROCK1, ROCK2 and LIMK1 were significantly decreased ($P < 0.01$) and cofilin was remarkably increased ($P < 0.05$) in CCG-1423-treatment GES-1 cells compared to those in untreated GES-1 cells, and the same trends were observed in NSC23766-treatment GES-1 cells after *H. pylori* infection compared to those in *H. pylori*-infected GES-1 cells (Fig. 6a). The protein phosphorylation levels of PAK1, ROCK2 and LIMK1 were significantly higher ($P < 0.05$), and cofilin was remarkably lower ($P < 0.05$) in GES-1 cells after *H. pylori* infection than those in untreated GES-1 cells. The protein phosphorylation levels of PAK1 and LIMK was significantly decreased, cofilin protein phosphorylation level was significantly increased in GES-1 cells treated with Rac1 inhibitor NSC 23766. The protein

phosphorylation levels of ROCK1, ROCK2 and LIMK was significantly reduced, cofilin protein phosphorylation level was significantly increased in GES-1 cells treated with the RhoA inhibitor CCG-1423 (Fig. 6b).

3. Discussion

The ability of *H. pylori* to regulate host autophagy is one of main pathogenic mechanism (Rubio et al., 2012). Autophagy can be employed as means of host defense and elimination of invasive bacteria at the initial stage; however, with the prolongation of exposure time, *H. pylori* can disrupt autophagy by preventing maturation of the autolysosome, leading to a chronic sense of bacterial persistent infections (Rubio et al., 2012). Although novel insights into the mechanism of autophagy in bacterial infection have emerged, many aspects remain largely unknown.

ILK, a serine/threonine kinase, is the key mediator of integrin signaling pathway and regulates cell migration, cell proliferation, and apoptosis (Dedhar, 2000). We found a negative correlation between ILK and LC3B in *H. pylori*-positive human samples (Fig. 1). This conclusion was further confirmed by an *in vitro* experiment, which demonstrated that total and phosphorylated ILK were downregulated, and the numbers of autophagosome and autolysome were increased in GES-1 cell lines after *H. pylori* infection (Fig. 2a-2d). As shown in Fig. 2a, CagA knockout *H. pylori* led lower level of ILK phosphorylation compared to that caused by *H. pylori* wild type, which indicated that ILK phosphorylation might be partly CagA-dependent pattern. The p62 levels decreased at 2 h and increased at 4, 6 and 8 h after *H. pylori* infection (Fig. 2e). The p62 is an adaptor protein that directs polyubiquitinated proteins to nascent autophagosomes, and disruption of autophagy results in the accumulation of p62 (Rubio et al., 2012). Tang et al. found that p62 was autophagic degraded in the initial stage of *H. pylori* infection. With the prolongation of *H. pylori* exposure time, the autophagy process was interrupted and p62 accumulated in cells (Kamm and Stull, 2001). These results together confirmed that ILK might be a critical regulator for *H. pylori*-induced autophagy.

To further study the influence of ILK on autophagy in *H. pylori*-infected GES-1 cells, RNAi was used to downregulate ILK level, and autophagy in GES-1 cells after *H. pylori* infection was then assessed. There was a significant accumulation of autophagosomes and increased LC3B levels both in *H. pylori*-infected and ILK-knockdown GES-1 cells (Fig. 3b-3e). The LC3B and p62 levels were both higher ($P < 0.05$) in ILK-knockdown GES-1 cells than those in control siRNA-treated GES-1 cells after *H. pylori* infection. These results point to ILK as a novel regulator of autophagy, related to *H. pylori* infection strategy. ILK had been known to associated with the cytoplasmic tail of the β1 integrin, which was first identified as a receptor of the *H. pylori* T4SS (Grashoff et al., 2012; Schuelein et al., 2011). The cytotoxin-associated genes pathogenicity island (cagPAI) encoded proteins to form a functional T4SS, and T4SS then delivered the virulence factors such as cagA into host target cells. Previous study had demonstrated that autophagy induction is independent on the cagPAI and T4SS (Deen et al., 2015; Terebiznik et al., 2009), thus further research on which component of *H. pylori* affected ILK and autophagy would be needed in the future.

ILK can activate the family members of Rho GTPases (Rac1 and RhoA), which mediate changes in actin polymerization, thus appearing to be specifically implicated in autophagy (Jang et al., 2012; Ivanovska et al., 2013; Xu et al., 2016). As shown in Fig. 4, Rac1 and RhoA activities were inhibited both in *H. pylori*-infected GES-1 cells and ILK-knockdown GES-1 cells regardless of whether or not GES-1 cells were infected with *H. pylori* (Fig. 5a and 5b). The results demonstrated that *H. pylori* reduced Rac1 and RhoA activities by affecting ILK levels. As shown in Fig. 5, inhibition of Rac1 or RhoA activities increased autophagosome and autolysosome formation in GES-1 cells. This indicated that the ILK/Rac1 and ILK/RhoA signaling pathways should affect autophagy in GES-1 cells.

Small GTP-binding proteins of the Rho family, such as Rac-1 and RhoA, can regulate the stability of newly formed actin filaments and actin dynamics by regulating downstream signal molecules (Ivanovska et al., 2013; Xu et al., 2016; Yuan et al., 2017). The Rho GTPase Rac1 can bind to and modulate the activation of PAK1 (Xu et al., 2014), which can also interact with LIMK1 to stabilize actin filament dynamics and inhibit downstream cofilin, an actin depolymerization agent (Hou et al., 2016). Cofilin-1 acts as a terminal effector of the Rho GTPases signaling cascade, which regulates actin dynamics by increasing the depolymerization of F-actin filaments (Wang et al., 2015). As shown in Fig. 6, the mRNA and protein phosphorylation levels of PAK1 and LIMK were significantly increased and mRNA and protein phosphorylation level of cofilin was significantly decreased in GES-1 cells after *H. pylori* infection. The results demonstrated that *H. pylori* activated Rac1/PAK1/LIMK1/cofilin signaling pathway in GES-1 cells. RhoA is the best-characterized Rho-associated coiled-coil containing kinases (ROCKs) regulators (Watanabe et al., 2015). ROCKs activation is accomplished by phosphorylation of several downstream target proteins to promote the formation of stress fibers (Watanabe et al., 2015). LIMK1 is also downstream of ROCKs, which phosphorylate and inactivate cofilin, thereby leading to a dynamic regulation of actin cytoskeleton (Ivanovska et al., 2013). There are two mammalian ROCK homologs, namely ROCK1 and ROCK2. Activated ROCK1 binds and phosphorylates to Beclin1 at Thr119 site to promote autophagy. Gurkar et al. showed that mice knocked out of ROCK1 gene resulted in impaired autophagy and reduced autophagosome formation (Zhang et al., 2018). In this study, ROCK1 and ROCK2 mRNA levels were significantly up-regulated, and ROCK1 phosphorylation levels were no obvious change in GES-1 cells after *H. pylori* infection. the mRNA and protein phosphorylation levels of ROCK1, ROCK2 and LIMK were significantly reduced and mRNA and protein phosphorylation level of cofilin was significantly increased in GES-1 cells treated with the RhoA inhibitor CCG-1423 (Fig. 6); this indicated that RhoA could control ROCK1/ROCK2/LIMK1/cofilin signaling pathway in *H. pylori*-infection GES-1 cells.

4. Conclusion

In summary, ILK could be a novel regulator of autophagy related to *H. pylori* infection strategy. We found a negative correlation between ILK and LC3B in *H. pylori*-positive human samples and *H. pylori*-infected GES-1 cell lines. Low expression of ILK targeted Rac1 and RhoA to induce autophagosome formation, and inhibited autophagy flux in GES-1 cells. Thus, *H. pylori* regulated ILK to disrupt autophagy through Rac1 and RhoA signaling pathways in gastric epithelial cells.

5. Materials And Methods

5.1 Reagents, antibodies and commercial kits

Primary antibodies we used were anti-LC3B (ab192890), anti-SQSTM1/p62 (ab56416), anti-Rac1 (ab33186), anti-RhoA (ab187027), anti-phospho-PAK1 (T212) (ab75599), anti-phospho-ROCK1 (T455 + S456) (ab203273), anti-ROCK2 (ab125025), anti-phospho-ROCK2 (ab228008), anti-LIMK1(ab81046), anti-phospho-LIMK1 (ab38508), anti-GAPDH (ab181602) from Abcam, and anti-ILK1 (#3856), anti-PAK1(#2602) anti-ROCK1(#4035), anti-cofilin1(#5175), anti-phospho-cofilin1 (#3313) from Cell Signaling Technology and anti-phospho-ILK1 (SAB,#12444) for western blot; anti-LC3B (ab48394) and anti-ILK (ab76468) from Abcam for confocal microscopy. Secondary antibodies included anti-mouse conjugated to horseradish peroxidase (Abcam, ab6789) and anti-rabbit conjugated to horseradish peroxidase (Cell Signaling Technology, #7074) were used for western blot; anti-rabbit conjugated to Dylight 488 (Abbkine, #A23220) and anti-mouse conjugated to Dylight 568 or Dylight 488 (Abbkine, #A23310 or #A23210) were for confocal microscopy.

Other agents: HBAD-mRFP-GFP-LC3-adenovirus were purchased from Hanbio. ILK siRNAs were from Invitrogen. Inhibitor of Rac1 (NSC23766) and RhoA (CCG-1423) were purchased from Selleck. Cell Counting Kit-8 was from Meilunbio. RhoA/Rac1/Cdc42 Combo Activation Assay kit (ab211168) was from Abcam. Transcriptor fist strand cDNA synthesis kit was purchased from Roche. BCA protein assay kit and chemiluminescence detection kit were both from Beyotime. Lipofectamine RNAiMAX Transfection kit was purchased from Invitrogen.

5.2 Clinical specimens

Eighteen *H. pylori*-positive and Nighteen *H. pylori*-negative gastric tissues were collected form patients at the Yantai Affiliated Hospital of Binzhou Medical University (Yantai, China). The diagnoses were based on clinical and histological laboratory examination.

5.3 Immunofluorescence for LC3B and ILK

Clinical samples of human stomach sections stored in paraformaldehyde were dehydrated, embedded in paraffin, sliced (Greenfield, Jones, 2013). Slides were treated with 3% H_2O_2 for 30 minutes and blocked with sheep serum for 1 h. The slides were incubated with primary antibody (anti-LC3B or anti-ILK, respectively) and a secondary fluorescent antibody, and then the nuclei were stained by DAPI. Sections were evaluated using laser scanning confocal microscopy (Zeiss MIC-SYSTEM). On randomly selected images of gastric epithelial cells ($n \geq 180$), the average fluorescence intensity of LC3B and ILK signals in human biopsies was measured by the software ZEN 2.5 lite of confocal microscopy.

5.4 Human gastric epithelial cells

The GES-1 cell lines maintained in Dulbecco Modified Essential Medium (DMEM) with 10% fetal bovine serum (FBS) under a humidified atmosphere of 5% CO_2 at 37˚C. When cells reached approximately

70%-90% confluence in 6-well plates, cells were treated with 0.25% trypsin and passaged (Zhang et al., 2016).

5.5 Co-culture of GES-1 cells with *H. pylori*

H. pylori strain 26695 was from the *H. pylori* Research Laboratory of the Chinese Center for Disease Control and Prevention (Beijing, China). Bacteria were grown on chocolate agar plate supplemented with 5% sheep's blood at 37 ˚C under microaerophilic conditions (85% N_2, 10% CO_2 and 5% O_2) (Zhang et al., 2016). GES-1 cells were plated onto 6-well plates in Dulbecco Modified Essential Medium (DMEM) with 10% fetal bovine serum (FBS) overnight, and then co-cultured with *H. pylori* at a multiplicity of infection (MOI) of 1:100 for 0, 2, 4, 6 and 8 h. GES-1 cells were immediately used to detect total ILK, phosphorylated ILK and p62 expression by western blot analysis and LC3B expression by mRFP-GFP-LC3B-Adenovirus transfection.

5.6 Western blot analysis

The GES-1 cells were lysed with 50 μL cell lysis buffer [RIPA (50 mM Tris pH 7.4, 0.1% SDS, 1% TritonX-100, 150 mM NaCl, 1 mM EDTA):PMSF = 16:1]. BCA Protein Assay Kit was used to determine the protein content. The 40 mg total protein was carried out by 12% SDS polyacrylamide gel electrophoresis and transferred to the polyvinylidene difluoride (PVDF) membrane. The membranes were incubated overnight with the primary antibody at 4 ˚C, and then incubated with secondary antibody at room temperature for 2 h. According to the manufacturer's instruction, the blots were detected with an enhanced chemiluminescence detection kit. GAPDH was used as control. ImageJ soft-ware was used to quantify the bands intensities (Zhang et al., 2017).

5.7 Adenovirus transfection

For transfection of mRFP-GFP-LC3B adenovirus, GES-1 cells were grown on coverslips at a density of 1.0×10^5 cells/well in Opti-MEM. The adenovirus was transfected into GES-1 cells (MOI = 100:1) for 12 h at 37 ˚C, and then maintained in DMEM for 48 h. Cells were washed three times with PBS and fixed with 4% of paraformaldehyde. Samples were analyzed for merge of GFP-LC3B and mRFP-LC3B (yellow), and mRFP-LC3B (red) puncta on confocal microscope at 40× (Tang et al., 2012). The numbers of yellow spots (autophagosome) and red spots (autolysosome) were calculated. During this experiment, adenovirus was first transfected into cells for 12 h, and ILK siRNA was used to interfere with the expression of ILK for 48 h, and then co-cultured with *H. pylori* for 6 h to observe the distribution of fluorescent spots in the cells.

5.8 Knockdown of ILK in GES-1 cells co-cultured withH. pylori

RNA interference (RNAi) was performed as previously described (Zhang et al., 2017). Briefly, knockdown of ILK was performed using siRNAs of HSS140843, HSS179923 and HSS179924 (Table 1). GES-1 were transfected with 100 nmol L^{-1} ILK siRNA using a Lipofectamine RNAiMAX Transfection kit according to the manufacturer's protocol. Briefly, 1.0×10^5 GES-1 cells/well were mixed with 2.5 μL ILK siRNA and

7.5 μL Lipofectamine RNAiMAX into 500 μL serum-free DMEM were co-cultured at 37 ˚C for 48 h in a humidified atmosphere of 5% CO_2. The GES-1 cells with control siRNA were used as the negative group. Western blot was employed to detect the effect of ILK knockdown according to the previous methods.

H. pylori were harvested and quantified using a spectrophotometer; quantities reached 1.0×10^8 CFU mL^{-1}. The GES-1 cells, GES-1 cells with control siRNA, and GES-1 cells transfected with ILK siRNA (HSS140843) were respectively seeded at a density of 1.0×10^5 cells/well, and then were incubated with the *H. pylori* at a multiplicity of infection of 1:100. The untreated GES-1 cells were as the blank group. The control siRNA transfected GES-1 cells were considered to be the negative group. The ILK siRNA transfected GES-1 cells were used as the siRNA group. The cells were then harvested after 6 h and assessed for adenovirus transfection, transmission electron microscopy, western blot. In order to determine whether ILK reduction was CagA-dependent after *H. pylori* infection, the GES-1 cells were co-cultured with CagA-knockout *H. pylori* ($CagA^-$) and wild-type *H. pylori* ($CagA^+$). The cells were then harvested after 6 h for western blot.

5.9 Transmission electron microscopy

For the transmission electron microscopy (TEM) to analyze autophagosomes and autolysosome, GES-1 cells were fixed in 2.5% glutaraldehyde at 4 ˚C for overnight. The GES-1 cells were washed three times with PBS ($0.1 mol \cdot L^{-1}$, pH 7.2) and then fixed again in 1% osmium acid solution for 1.5 h, which were dehydrated in gradient ethanol, embedded in Epon. The Epon was cut into ultrathin sections with a thickness of 70 nm, and then it was dyed with 2% uranium dioxide acetate solution in dark for 20 min, and then dyed again with lead citrate solution for 7 min. Observation and photography of cells were used by transmission electron microscopy (Hitachi HT-7800) at 80 kV (Dejaeger et al., 2017).

5.10 Cell survival rate assays

Cell survival rates were assessed using Meilun Cell Counting Kit-8 (Meilunbio, China) according to the manufacturer's instructions. Briefly, the GES-1 cells were seeded on a 96-well plate at a concentration of 5×10^3 cells per well. The GES-1 cells were treated with Rac1 inhibitor NSC23766 (10, 50, 100 and 200 μM) or RhoA inhibitor CCG-1423 (2, 5, 10 and 25 μM) for 2 h in an incubator at 37 °C in 5% CO_2 to detect concentration-dependent toxicity of inhibitors. The GES-1 cells were treated with 50 μM of NSC23766 or 5 μM of CCG-1423 at 1, 2, 4, 8 and 12 h in an incubator at 37 °C in 5% CO_2 to detect time-dependent toxicity of inhibitors. After treatment duration, the CCK-8 assay reagent was added to culture media and incubated for 2 h. Absorbance was read at 450 nm on a multifunctional microplate reader (Wang et al., 2019).

5.11 RhoA and Rac1 activation assay

RhoA and Rac1 activation assays were measured using RhoA/Rac1/Cdc42 Combo Activation Assay Kit (Abcam, ab211168) according to the manufacturer's instructions. Briefly, the GES-1 cells were lysed in

cold lysis buffer containing protease inhibitor for 20 min. Thereafter, they were centrifuged at 14,000 × g for 10 min at 4 °C, and the supernatant was then for measurement of RhoA and Rac1 kinase activity. 40 µL of Rhotekein RBD beads or PAK1 PBD beads were separately added to the supernatant for 1 h at 4 °C to bind to GTP-RhoA or GTP-Rac1, and then centrifuged at 14,000 × g for 10 s at 4 °C. Mixture of the supernant and 5 × SDS-PAGE sample buffer was boiled at 100 °C for 10 min as total RhoA or Rac1 (T-RhoA or T-Rac1). The pellet was washed three times with 0.5 mL of 1 × Assay Buffer, resuspended in 40 µL of 2 × SDS-PAGE sample buffer and then boiled at 100 °C for 10 min. Thereafter, they were centrifuged at 14,000 × g for 10 s at 4 °C, and the supernatant was used as active RhoA or Rac1 (GTP-RhoA or GTP-Rac1). The active and total RhoA, or active and total Rac1 were analyzed by western blot (Barbati et al., 2015).

5.12 Drug treatment in GES-1 cells co-cultured withH. pylori

The Drugs NSC 23766 or CCG-1423 were used as inhibitors of Rac1 or RhoA, which was dissolved in 10% DMSO and diluted with Opti-MEM. Briefly, GES-1 cells were grown at a density of 1.0×10^5 cells/well in Opti-MEM and treated with either NSC 23766 (50 µM) (Maekawa et al., 1999) or CCG-1423 (5 µM) (Montani et al., 2009) for 2 h. The untreated GES-1 cells were employed the blank group. *H. pylori* were added to the cells at a multiplicity of infection of 100:1. The cells were then harvested after 6 h and assessed for adenovirus transfection, western blot and real-time PCR.

5.13 Quantification of ROCK1, ROCK2, PAK1, LIMK1 and cofilin1 by quantitative real-time RT-PCR

The ROCK1, ROCK2, PAK1, LIMK1 and cofilin1 mRNA expression in GES-1 were detected by quantitative real-time polymerase chain reaction (RT-PCR). The SYBR Green RT-PCR assay was performed in an ABI PRISM 7500 Sequence Detection System (ThermoFisher Scientific, USA). The amplifications were conducted in 20 µL using the following thermal profile: 95 °C for 3 min, followed by 40 cycles at 95 °C for 15 s and 58 °C for 33 s. The ROCK1-specific primers ROCK1-F and ROCK1-R, ROCK2-specific primers ROCK2-F and ROCK2-R, PAK1-specific primers PAK1-F and PAK1-R, LIMK1-specific primers LIMK1-F and LIMK1-R, cofilin1-specific primers CFL1-F and CFL1-R and GAPDH-specific primers GAPDH-F and GAPDH-R (Table 1), were used to amplify the corresponding products. The comparative average-cycle threshold method was used to analyze ROCK1, ROCK2, PAK1, LIMK1 and cofilin1 mRNA levels, which could be calculated with an n-fold difference relative to the GAPDH (Zhu et al., 2012).

5.14 Statistical analysis

Data are presented as mean ± standard deviations (SD) from at least five independent experiments. Pearson correlation coefficient was used to study the relationship between LC3B and ILK in clinical

samples. All data were subjected to one-way analysis of variance. $P \leq 0.05$ was considered statistically significant.

6. Declarations

6.1 Ethics approval and consent to participate

Informed consent for study has been obtained from all patients. The present study was sanctioned by the ethics committees of Binzhou Medical University.

6.2 Consent for publication

Not applicable.

6.3 Availability of data and materials

The datasets used and/or analysed during the current study are available from the corresponding author on reasonable request.

6.4 Competing interests

The authors declare that they have no competing interests.

6.5 Funding

This work was supported by grants from the National Natural Science Foundation of China (grant numbers: 81771709 and 81471561); Department of Education of Shandong Province (2019KJK012).

6.6 Authors's contributions

YZ and BL were major contributors in project administration, funding acquisition and writing—review and editing. ZX was a major contributor in methodology, data curation and writing—original draft preparation. YD, RZ and XT performed formal analysis and investigation. YW and XJ performed western blot assays.

6.7 Acknowledgements

Not applicable.

7. References

Barbati C, Alessandri C, Vomero M, Vona R, Colasanti T, Vacirca D. Autoantibodies specific to D4GDI modulate Rho GTPase mediated cytoskeleton remodeling and induce autophagy in T lymphocytes. J Autoimmun. 2015;58:78-89.

Churin Y, Kardalinou E, Meyer TF, Naumann M. Pathogenicity island-dependent activation of Rho GTPases Rac1 and Cdc42 in *Helicobacter pylori* infection. Mol Microbiol. 2001;40:815-23.

Dedhar S. Cell-substrate interactions and signaling through ILK. Curr Opin Cell Biol. 2000;12:250-6.

Deen NS, Gong L, Naderer T, Devenish RJ, Kwok T. Analysis of the relative contribution of phagocytosis, LC3-associated phagocytosis, and canonical autophagy during *Helicobacter pylori* infection of macrophages. Helicobacter 2015;20:449-59.

Dejaeger M, Böhm AM, Dirckx N, Devriese J, Nefyodova E, Cardoen R. et al. Integrin-linked kinase regulates bone formation by controlling cytoskeletal organization and modulating BMP and Wnt Signaling in Osteoprogenitors. J Bone Miner Res. 2017;32:2087-102.

Dunn BE, Cohen H, Blaser MJ. *Helicobacter pylori*. Clin Microbiol Rev. 1997;10:720-41.

Ghatak S, Morgner J, Wickström SA. ILK: a pseudokinase with a unique function in the integrin-actin linkage. Biochem Soc Trans. 2013;41:995-1001.

Graness A, Giehl K, Goppelt-Struebe M. Differential involvement of the integrin-linked kinase (ILK) in RhoA-dependent rearrangement of F-actin fibers and induction of connective tissue growth factor (CTGF). Cell Signal. 2006;18:433-40.

Grashoff C, Thievessen I, Lorenz K, Ussar S, Fässler R. Integrin-linked kinase: integrin's mysterious partner. Curr Opin Cell Biol. 2004;16:565-71.

Greenfield LK, Jones NL. Modulation of autophagy by *Helicobacter pylori* and its role in gastric carcinogenesis. Trends Microbiol. 2013;21:602-12.

Gurkar AU, Chu K, Raj L, Bouley R, Lee SH, Kim YB, et al. Identification of ROCK1 kinase as a critical regulator of Beclin1-mediated autophagy during metabolic. Nat Commun. 2013;4:2189.

Hou X, Liu J, Zhang Z, Zhai Y, Wang Y, Wang Z, et al. Effects of cytochalasin B on DNA methylation and histone modification in parthenogenetically activated porcine embryos. Reproduction 2016;152:519-27.

Ivanovska J, Tregubova A, Mahadevan V, Chakilam S, Gandesiri M, Benderska N, et al. Identification of DAPK as a scaffold protein for the LIMK/cofilin complex in TNF-induced apoptosis. Int J Biochem Cell Biol. 2013;45:1720-9.

Jang I, Jeon BT, Jeong EA, Kim EJ, Kang D, Lee JS, et al. Pak1/LIMK1/Cofilin pathway contributes to tumor migration and invasion in human non-small cell lung carcinomas and cell lines. Korean J Physiol Pharmacol. 2012;16:159-65.

Kalwat MA, Yoder SM, Wang Z, Thurmond DC. A p21-activated kinase (PAK1) signaling cascade coordinately regulates F-actin remodeling and insulin granule exocytosis in pancreatic β cells. Biochem.

Pharmacol. 2013;85:808-16.

Kamm KE, Stull JT. Dedicated myosin light chain kinases with diverse cellular functions. J Biol Chem. 2001;276:4527-30.

Kast DJ, Dominguez R. The cytoskeleton-autophagy connection. Curr Biol. 2017;27: R318-R326.

Klionsky DJ, Cregg JM, Dunn WA Jr, Emr SD, Sakai Y, Sandoval IV, et al. A unified nomenclature for yeast autophagy-related genes. Dev Cell. 2003;5:539-45.

Klionsky DJ, Emr SD. Autophagy as a regulated pathway of cellular degradation. Science 2000;290:1717-21.

Otero LL, Ruiz VE, Perez GI. *Helicobacter pylori*: the balance between a role as colonizer and pathogen. Best Pract Res Clin Gastroenterol. 2014;28:1017-29.

Maekawa M, Ishizaki T, Boku S, Watanabe N, Fujita A, Iwamatsu A, et al. Signaling from Rho to the actin cytoskeleton through protein kinases ROCK and LIM-kinase. Science 1999;285:895-8.

Montani L, Gerrits B, Gehrig P, Kempf A, Dimou L, Wollscheid B, et al. Neuronal Nogo-A modulates growth cone motility via Rho-GTP/LIMK1/cofilin in the unlesioned adult nervous system. J Biol Chem. 2009;284:10793-807.

Radosz-Komoniewska H, Bek T, Jóźwiak J, Martirosian G. Pathogenicity of *Helicobacter pylori* infection. Clin Microbiol Infect. 2005;11:602-10.

Raju D, Hussey S, Ang M, Terebiznik MR, Sibony M, Galindo-Mata E, et al. Vacuolating cytotoxin and variants in Atg16L1 that disrupt autophagy promote *Helicobacter pylori* infection in humans. Gastroenterology 2012;142:1160-71.

Rich KA, Burkett C, Webster P. Cytoplasmic bacteria can be targets for autophagy. Cell Microbiol. 2003;5:455-68.

Rubio MD, Haroutunian V, Meador-Woodruff JH. Abnormalities of the Duo/Rac-1/PAK1 pathway drive myosin light chain phosphorylation in frontal cortex in schizophrenia. Biol Psychiatry. 2012;71:906-14.

Schuelein R, Everingham P, Kwok T. Integrin-mediated type IV secretion by Helicobacter: what makes it tick? Trends Microbiol. 2011;19:211-6.

Sit WY, Chen YA, Chen YL, Lai CH, Wang WC. Cellular evasion strategies of *Helicobacter pylori* in regulating its intracellular fate. Semin. Cell Dev Biol. 2020;101:59-67.

Tang B, Li N, Gu J, Zhuang Y, Li Q, Wang HG, et al. Compromised autophagy by MIR30B benefits the intracellular survival of *Helicobacter pylori*. Autophagy 2012;8:1045-57.

Terebiznik MR, Raju D, Vázquez CL, Torbricki K, Kulkarni R, Blanke SR, et al. Effect of *Helicobacter pylori*'s vacuolating cytotoxin on the autophagy pathway in gastric epithelial cells. Autophagy 2009;5:370-9.

Wang G, Pang J, Hu X, Nie T, Lu X, Li X, et al. Daphnetin: a novel anti-*Helicobacter pylori* agent. Int J Mol Sci. 2019;20:850.

Wang YH, Wu JJ, Lei HY. When *Helicobacter pylori* invades and replicates in the cells. Autophagy 2009;5:540-2.

Wang Y, Kunit T, Ciotkowska A, Rutz B, Schreiber A, Strittmatter F, et al. Inhibition of prostate smooth muscle contraction and prostate stromal cell growth by the inhibitors of Rac, NSC23766 and EHT1864. Br J Pharmacol. 2015;172:2905-17.

Watanabe B, Minami S, Ishida H, Yoshioka R, Nakagawa Y, Morita T, et al. Stereospecific inhibitory effects of CCG-1423 on the cellular events mediated by myocardin-related transcription factor A. PLoS One 2015;10:1-16.

Xu B, Bai B, Sha S, Yu P, An Y, Wang S, et al. Interleukin-1β induces autophagy by affecting calcium homeostasis and trypsinogen activation in pancreatic acinar cells. Int J Clin Exp Pathol. 2014;7:3620-31.

Xu S, Guo X, Gao X, Xue H, Zhang J, Guo X, et al. Macrophage migration inhibitory factor enhances autophagy by regulating ROCK1 activity and contributes to the escape of dendritic cell surveillance in glioblastoma. Int J Oncol. 2016;49:2105-15.

Yuan D, Zhao Y, Wang Y, Che J, Tan W, Jin Y, et al. Effect of integrin-linked kinase gene silencing on microRNA expression in ovarian cancer. Mol Med Rep. 2017;16:7267-76.

Zeng LH, Xu L, Rensing NR, Sinatra PM, Rothman SM, Wong M. Kainate seizures cause acute dendritic injury and actin depolymerization *in vivo*. J Neurosci. 2007;27:11604-13.

Zhang H, Yao X, Ding Y, Xu Z, Liang R, Zhang Y, et al. PI3K signaling pathways modulated white spot syndrome virus (WSSV) replication in *Procambarus clarkii*. Fish Shellfish Immunol. 2018;76:279-86.

Zhang Y, Sun H, Chen X, Li J, Zhao H, Geng L, et al. Functional profile of gastric epithelial cells infected with *Helicobacter pylori* strains. Microb Pathog. 2016;95: 77-81.

Zhang Y, Sun H, Li J, Rong Q, Ji X, Li B. The leukocyte-associated immunoglobulin (Ig)-like receptor-1 modulating cell apoptosis and inflammatory cytokines secretion in THP-1 cells after *Helicobacter pylori* infection. Microb Pathog. 2017;109:292-9.

Zhu G, Wang Y, Huang B, Liang J, Ding Y, Xu A, et al. A Rac1/PAK1 cascade controls β-catenin activation in colon cancer cells. Oncogene. 2012;31:1001-12.

8. Table

Table 1. Names and sequences of ILK siRNA and primers used in the study

Primer Name	Primer Sequences
ILK (HSS140843)	F 5′-GCCUGUGGCUGGACAACACGGAGAA-3′
	R 5′-UUCUCCGUGUUGUCCAGCCACAGGC-3′
ILK (HSS179923)	F 5′-CAGCCAGUCAUGGACACCGUGAUAU-3′
	R 5′-AUAUCACGGUGUCCAUGACUGGCUG-3′
ILK (HSS179924)	F 5′-GCAUUGACUUCAAACAGCUUAACUU-3′
	R 5′-AAGUUAAGCUGUUUGAAGUCAAUGC-3′
PAK1 (GeneID 5058)	F 5′-ACCACTCCACCAGATGCTTTGAC-3′
	R 5′-TTCTTAGGATCGCCCACACTCAC-3′
ROCK1 (GeneID 6093)	F 5′-CTGCAACTGGAACTCAACCAAGAA-3′
	R 5′-GCTGGCCAACTGCATCTGAA-3′
ROCK2 (GeneID 9475)	F 5′-AGCTGCGGTCACAACTCCAA-3′
	R 5′-TGTTGTTTCGTACAGGCAATGAAAG-3′
LIMK1 (GeneID 3984)	F 5′-CCCAACGTGCTCAAGTTCATC-3′
	R 5′-GTCCTTGGCAAAGCTCACTCTC-3′
CFL1 (GeneID 1072)	F 5′-CCAGATAAGGACTGCCGCTATG-3′
	R 5′-TCGTAGCAGTTTGCTTGCAATTC-3′
GAPDH (GeneID 2597)	F 5′-GCACCGTCAAGGCTGAGAAC-3′
	R 5′-TGGTGAAGACGCCAGTGGA-3′

Figures

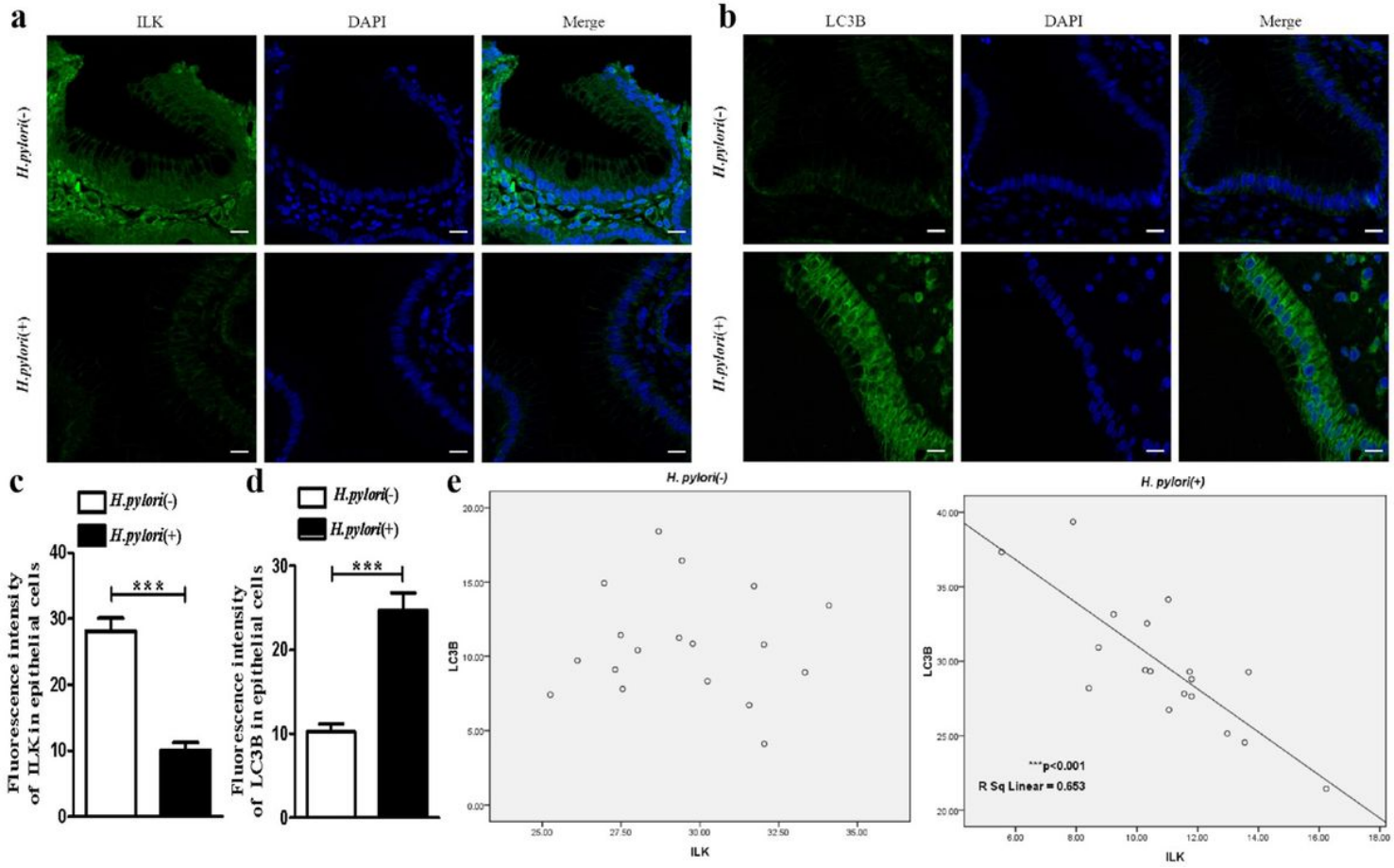

Figure 1

ILK and LC3B levels in clinical samples of human stomach tissue. (a) Immunostaining for ILK in clinical samples of human stomach tissue. Green color indicates ILK staining. Nuclei (blue color) were stained with DAPI. Scale bar: 20 μm. (b) Immunostaining for LC3B in clinical samples of human stomach tissue. Green color indicates LC3B staining. Nuclei (blue color) were stained with DAPI. Scale bar: 20 μm. (c) Fluorescence intensity of ILK in clinical samples of human stomach tissue with or without H. pylori infection. ***P < 0.001. (d) Fluorescence intensity of LC3B in clinical samples of human stomach tissue with or without H. pylori infection. ***P < 0.001. (e) Pearson's correlation coefficient to study the relationship between LC3B and ILK in clinical samples.

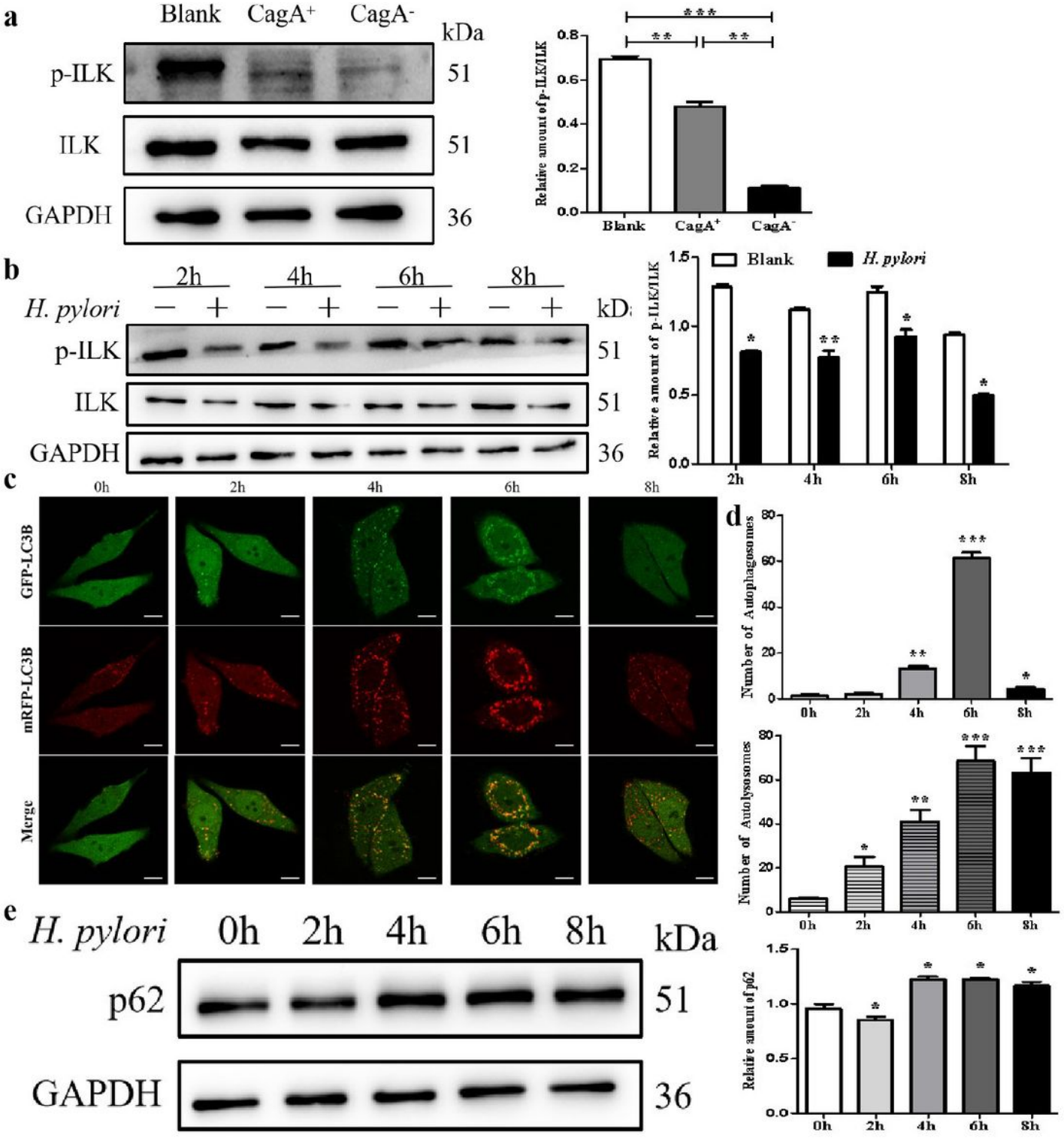

Figure 2

The ILK and the LC3B levels in GES-1 cells after H. pylori infection. (a) Western blot analysis to total and phopshorylated ILK in GES-1 cells after H. pylori infection with or without CagA. Data are presented as mean ± SD of five independent assays. **P < 0.01, ***P < 0.001. (b) Western blot analysis to detect total and phopshorylated ILK at 0, 2, 4, 6, and 8 h in GES-1 cells after H. pylori infection. Data were presented as mean ± SD of 5 independent assays. Asterisks indicate significant difference compared to thosein

untreated GES-1 cells (*P < 0.05, **P < 0.01). (c) Cells were transiently transfected with an mRFP-GFP tandem fluorescent-tagged LC3B (mRFP-GFP-LC3B) at 0, 2, 4, 6, and 8 h. (d) The numbers of yellow spots (autophagosome) and red spots (autolysosome) were calculated at 0, 2, 4, 6, and 8 h in GES-1 cells. Asterisks indicate significant difference compared to that at 0 h (*P < 0.05, **P < 0.01, ***P < 0.001). (e) Western blot analysis to detect p62 at 0, 2, 4, 6, and 8 h in GES-1 cells after H. pylori infection. Data were presented as mean ± SD of 5 independent assays. Asterisks indicate significant difference compared to that at 0 h (*P < 0.05).

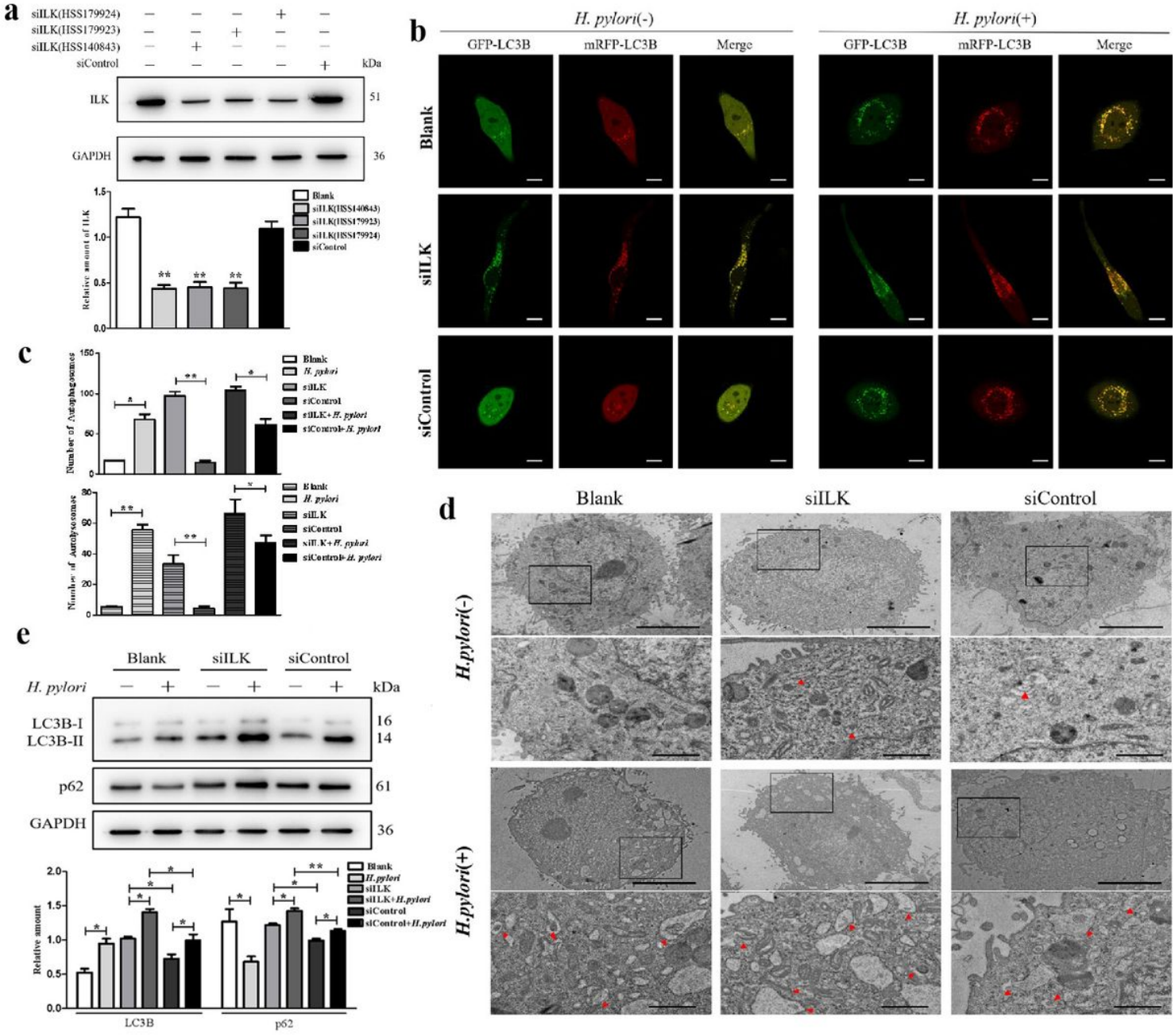

Figure 3

Downregulation of ILK influenced autophagy in GES-1 cells. (a) Western blot analysis to detect ILK expression at 48 h in GES-1 cells after transfection with sequence-specific siRNA (HSS140843, HSS179923, or HSS179924) targeting ILK. Data are presented as mean ± SD of five independent assays.

Two asterisks indicate significant difference compared to that treated with control siRNA (siControl). (b) GES-1 cells, which had been transfected with mRFP-GFP-LC3B adenovirus for 12 h, were transfected with control siRNA (siControl) or ILK siRNA (siILK) for 48 h and then infected with or without H. pylori for 6 h. Scale bar: 10 μm. (c) The number of autophagosome and autolysosome was calculated. Data are presented as mean ± SD of 30 cells. (d) Ultrastructural features of GES-1 cells were analyzed by transmission electron microscopy. Ultrastructural features of H. pylori-uninfected and H. pylori-infected GES-1 cells are shown in the first and third lines, respectively. Scale bar: 5 μm. The typical images of autophagosomes (red arrow) in the second and fourth lines are shown at higher magnification according to ultrastructural features of the first and third lines, respectively. Scale bar: 1 μm. (e) Western blot analysis to detect LC3B and p62 in blank, siControl- or siILK-treatment GES-1 cells infected with or without H. pylori for 6 h. Data are presented as mean ± SD of five independent assays (*P < 0.05, **P < 0.01).

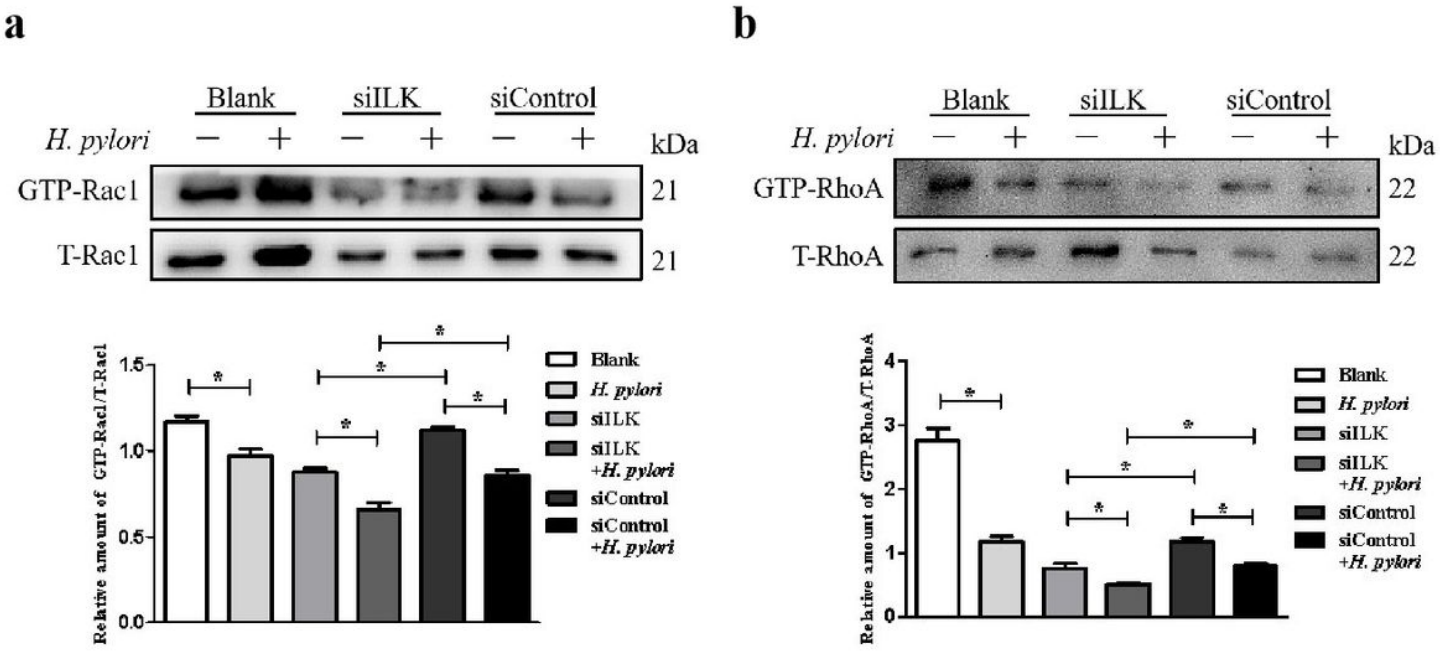

Figure 4

The Rac1 and Rho activation assay in the GES-1 cells. The GTP-Rac1/T-Rac1 (a) and GTP-RhoA/T-RhoA (b) levels in ILK-knockdown GES-1 cells after H. pylori infection through western blot analysis. Blank: The untreated GES-1 cells; siILK: The GES-1 cells were transfected with ILK siRNA; siControl: The GES-1 cells were transfected with control siRNA. The quantitative data are presented as means ± SD of 5 independent assays (*P < 0.05).

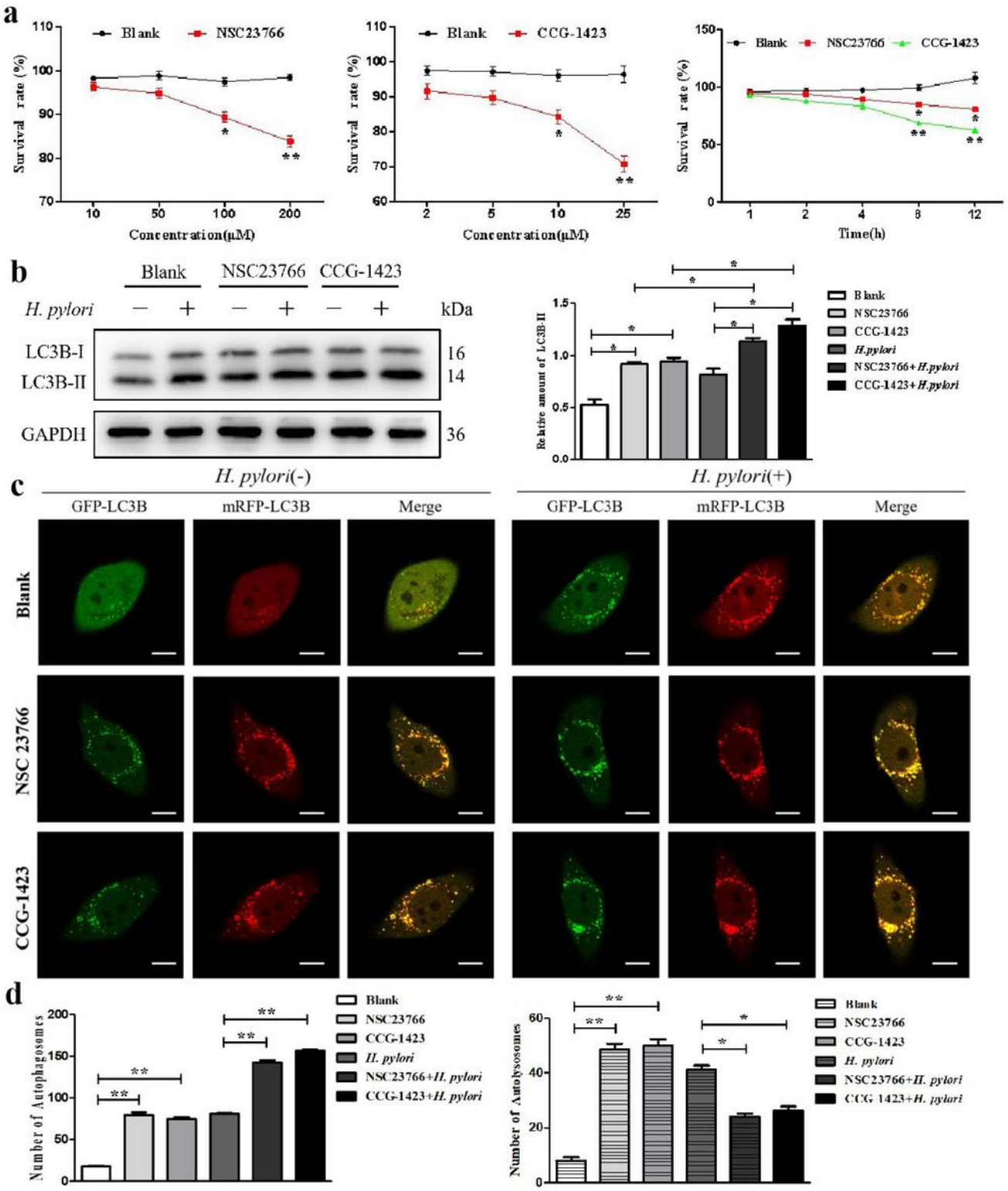

Figure 5

Inhibition of Rac1 and RhoA influenced autophagy in GES-1 cells. (a) CCK-8 to measure concentration and time-dependent toxicity of NSC 23766 and CCG-1423 to GES-1 cells. Asterisks indicate significant difference compared to blank (*P < 0.05, **P < 0.01). (c) LC3B protein levels detected by western blot analysis in GES-1 cells, H. pylori-infected GES-1 cells, GES-1 cells treated with NSC 23766 (50 μM), H. pylori-infected GES-1 cells treated with NSC 23766 (50 μM), GES-1 cells treated with CCG-1423 (5 μM),

and H. pylori-infected GES-1 cells treated with CCG-1423 (5 μM). The quantitative data are presented as mean ± SD of five independent assays (*P < 0.05). (d) GES-1 cells, which had been transfected with mRFP-GFP-LC3B adenovirus for 12 h, were treated with NSC 23766 (50 μM) or CCG-1423 (5 μM) for 6 h and then infected with or without H. pylori for 6 h. Scale bar: 10 μm. (e) The number of autophagosomes and autolysosomes was calculated. Data are presented as mean ± SD of 30 cells.

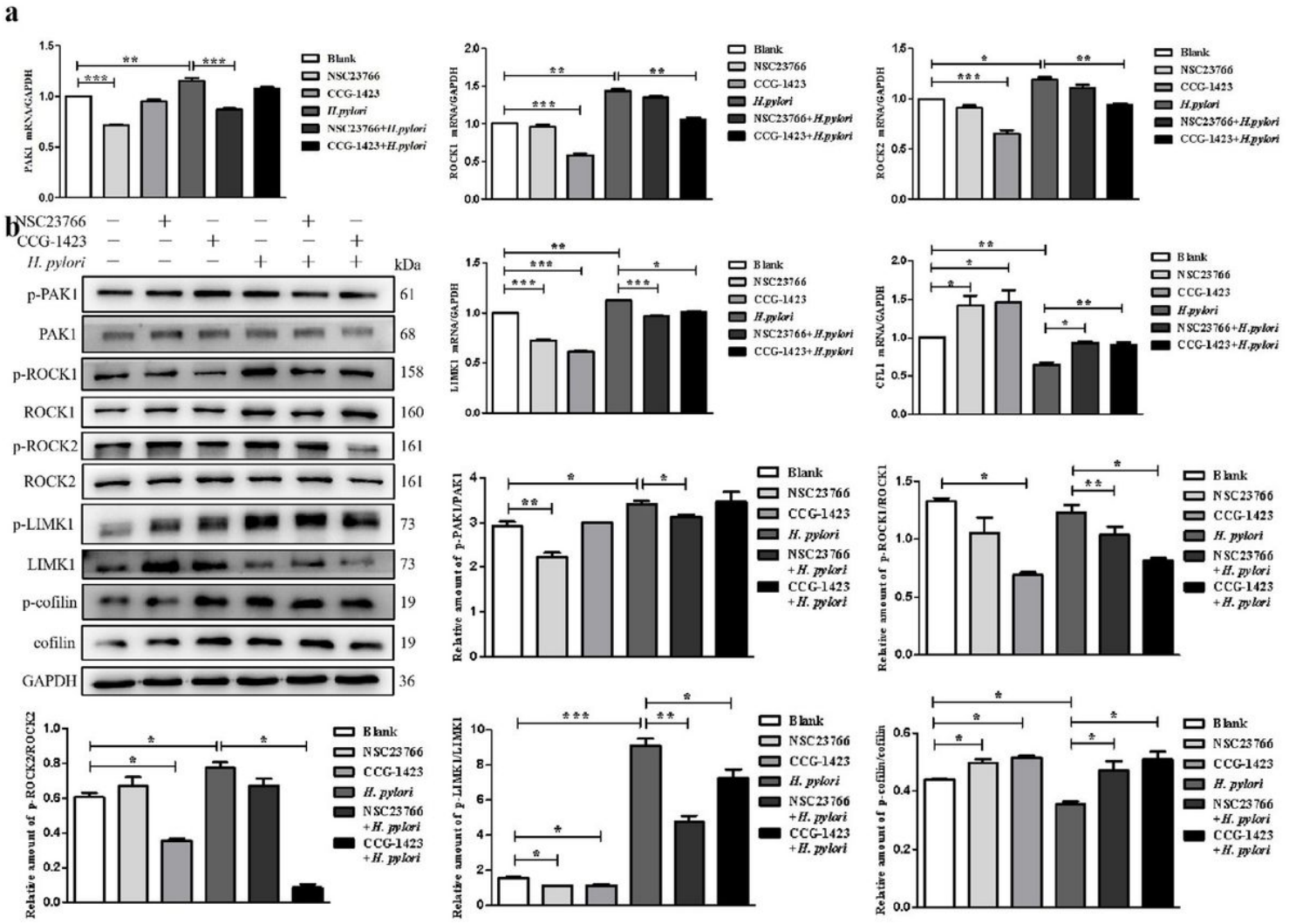

Figure 6

Inhibition of Rac1 and RhoA influenced downstream signaling pathway moleculars. (a) The mRNA levels, (b) phosphorylated and total protein levels of ROCK1, ROCK2, PAK1, LIMK1, and Cofilin1 was determined by quantitative RT-PCR and western blot in GES-1 cells, H. pylori-infected GES-1 cells, GES-1 cells treated with NSC 23766 (50 μM), H. pylori-infected GES-1 cells treated with NSC 23766 (50 μM), GES-1 cells treated with CCG-1423 (5 μM), and H. pylori-infected GES-1 cells treated with CCG-1423 (5 μM). The quantitative data are presented as mean ± SD of five independent assays (*P < 0.05; **P < 0.01; ***P < 0.001).